

Spin-triplet pairing in large nuclei

G.F. Bertsch and Y. Luo

Institute for Nuclear Theory and Dept. of Physics, University of Washington, Seattle, Washington

(Dated: 12/11/2009)

The nuclear pairing condensate is expected to change character from spin-singlet to spin-triplet when the nucleus is very large and the neutron and proton numbers Z, N are equal. We investigate the transition between these two phases within the framework of the Hartree-Fock-Bogoliubov equations, using a zero-range interaction to generate the pairing. We confirm that extremely large nucleus would indeed favor triplet pairing condensates, with the Hamiltonian parameters taken from known systematics. The favored phase is found to depend on the specific orbitals at the Fermi energy. The smallest nuclei with a well-developed spin-triplet condensate are in the mass region $A \sim 130 - 140$.

INTRODUCTION

The neutron-proton interaction in the spin-one channel is attractive and stronger than the identical-nucleon interaction. Nevertheless, the nuclei observed in nature favor identical-particle pairing. A trivial answer to this puzzle is that most nuclei have different numbers of protons and neutrons, and the isospin polarization discourages pairing in the isospin-zero ($T=0$) channel. But even in nuclei with equal numbers of neutron and protons the $J = 1, T = 0$ neutron-proton pairing does not compete well with ordinary $J = 0, T = 1$ pairing, as evidenced by the ground-state spins and binding systematics of odd-odd nuclei[1, 2]. This puzzle presents a serious challenge to nuclear theory that must be resolved if the theory is to be used confidently in contexts where experimental information is not available, such as astrophysical environments.

It has recently been suggested that the explanation of the suppressed spin-triplet pairing is the presence of the strong nuclear spin-orbit field [3, 4, 5, 6]. The spin-orbit field interferes with the pairing in both channels, but it suppresses it more strongly in the $J = 1$ neutron-proton channel than in the $J = 0$ identical-particle channel. Since the spin-orbit splitting is a surface effect, one might expect that the pairing would change character to the $J = 1$ condensate in extremely large nuclei. In the limit of large nuclear size, the surface-to-volume ratio would be small and the spin-orbit field would be ineffective at controlling the single-particle spectrum. In this paper we apply the Hartree-Fock-Bogoliubov (HFB) theory with a simplified Hamiltonian to examine the properties of the pairing condensate as one approach this limit. We shall find that the transition to $J = 1$ pairing does occur in large nuclei, but is only strong for nuclei that are somewhat beyond the limit of stability with respect to proton emission.

THE HAMILTONIAN

To keep the calculations as simple as possible, we consider a Hamiltonian consisting of a phenomenological single-particle Hamiltonian together with a two-particle interaction,

$$\hat{H} = \sum_i \langle i | H_{sp} | j \rangle a_i^\dagger a_j + \sum_{i>j, k>l} \langle ij | v | kl \rangle a_i^\dagger a_j^\dagger a_l a_k \quad (1)$$

Here the single-particle Hamiltonian H_{sp} is taken with the well-known Woods-Saxon form,

$$H_{sp} = \frac{p^2}{2m} + V_{WS} f(r) + \vec{\ell} \cdot \vec{s} V_{so} \frac{1}{r} \frac{df(r)}{dr} \quad (2)$$

with $f(r) = 1/(1 + \exp((r - R)/a))$ and R the radius of the potential. We use parameter values $V_{WS} = -50$ MeV, $a = 0.67$ fm which are close to standard values in the literature [7, Eq. 2.181]. We do not expect that the competition between the different kinds of pairing will depend sensitively on V_{WS} and a .

The spin-orbit strength parameter V_{so} will be important in the competition, and its determination requires some discussion. Unfortunately, first-principles studies of the nuclear Hamiltonian are not at a point where quantitatively reliable spin-orbit fields can be calculated [8]. However, given the Woods-Saxon form in Eq. (2), one can constrain the parameter quite well from spectroscopic data. A good source is the energies of single-particle excitations in nuclei adjacent to closed shells. For the present study we fit the experimental spin-orbit splitting of the $f_{7/2}$ and $f_{5/2}$ in the nucleus ^{41}Ca [9]. The measured value is 7.0 MeV, and the fitted spin-orbit strength is $V_{so} = 33$ MeV-fm². We estimate an uncertainty of not more than 10% in this value, based on comparison with other ways to estimate it.

We only treat nuclei with equal numbers of neutrons and protons in this work, enforcing the condition by taking equal chemical potential in the HFB equations. The value of the chemical potential is fixed by demanding that the density goes to the standard value $\rho = 0.16$

fm^{-3} in the nuclear-matter limit. With the chosen single-particle Hamiltonian, the corresponding chemical potential is $\lambda = -13$ MeV. Note that our Hamiltonian neglects the Coulomb interaction. This allows us to approach the nuclear matter limit but the calculated nuclei extend to the unphysical region beyond the proton dripline.

Interaction

The two-particle matrix elements are determined by a contact interaction of the general form

$$\langle ij|v|kl\rangle = \sum_{\alpha} v_{\alpha} \langle ij|\delta^{(3)}(\vec{r}-\vec{r}')P_{L=0}P_{\alpha}|kl\rangle. \quad (3)$$

Here $P_{L=0}$ is a projection operator on total orbital angular momentum zero. The P_{α} is a projection operator on the six spin-isospin channels $(S_{S_z}, T_{T_z}) = (0_0, 1_1), (0_0, 1_0), (0_0, 1_{-1}), (1_0, 0_0), (1_1, 0_0), (1_{-1}, 0_0)$. The interaction strengths v_{α} are of course independent of the z -projections of spin and isospin, and we shall call the two independent strengths v_s and v_t for spin-singlet and spin-triplet, respectively. However, we will need to keep explicit the six amplitudes with different z -projections when constructing the HFB condensate. It should also be noted that the contact interaction has to be regulated in some way to produce a finite condensate. This will be implemented by including only orbitals whose orbital single-particle energies ε_{ℓ} are within a range $E_B/2$ of the Fermi energy, $\lambda - E_B/2 < \varepsilon_{\ell} < \lambda + E_B/2$.

Our choices for the parameters will be guided by the relevant shell model matrix elements of phenomenological shell-model Hamiltonians. In this way we hope to avoid some of the ambiguity associated with the form of the pairing interaction (see concluding section). Specifically, we take the USDB Hamiltonian fitted to *sd*-shell nuclei [10] and the GX1A Hamiltonian fitted to *fp* shell nuclei [11]. We consider all the shell-model matrix elements with total spin and isospin couplings $(J, T) = (0, 1), (1, 0)$, and make a least-squares fits to each set using the contact interaction and harmonic oscillator orbitals. In the fit, we give equal weight to all matrix elements in the m -scheme representation. The results for the ratio of interactions strengths v_t/v_s , shown in Table I, are in the range 1.6-1.7. Another fitted Hamiltonian to *fp*-shell spectra [3] gives a very similar ratio (1.56). To get the absolute values of the strengths, we also need to specify the oscillator parameter controlling the size of the orbitals. This is taken as $\hbar\omega = 14$ MeV and 11 MeV for the *sd*-shell fit and the *fp*-shell fit respectively. The deduced strength parameters v_s, v_t are also given in the table. One sees that the interactions derived from USDB and GX1A are in good accord with each other. Unaccountably, the interaction from ref. [3] has much lower strengths. For application to the HFB theory outside

given shell-model spaces, it is still necessary to choose a suitable space cutoff parameter E_B . An argument can be made identifying E_B with the harmonic oscillator shell energy $\hbar\omega$, which would put it in the range of 11 – 14 MeV for the strengths in Table I. For our study here, we have somewhat arbitrarily taken the strength of the spin-singlet and spin-triplet interactions to be $v_s = 300$ MeV- fm^3 and $v_t = 450$ MeV- fm^3 , respectively, with a cutoff of $E_B = 10$ MeV. The ratio is 1.5, giving the spin-triplet somewhat less of an enhancement than the fits suggests. The calculations will then be on the conservative side in testing for a possible phase transition.

TABLE I: Strengths of triplet and singlet interactions from shell-model fits and their ratios. See text for details.

Source	v_s	v_t	Ratio
	MeV- fm^3	MeV- fm^3	
<i>sd</i> -shell [10]	280.	465.	1.65
<i>fp</i> -shell [11]	291.	475.	1.63

HFB

The physical quantity to be calculated is the energy of the system in a state constructed by making a Bogoliubov transformation on the noninteracting ground state. The expression for the energy is

$$E = \sum_{ij} \rho_{ij} \langle i|H_{sp}|j\rangle + \sum_{i>j} \sum_{i'>j'} \kappa_{ij} \langle ij|v|i'j'\rangle \kappa_{i'j'} \quad (4)$$

where ρ_{ij} and κ_{ij} are the ordinary and anomalous densities associated with the transformation. There is also a ρ^2 term in the interaction energy which we ignore along with all other Hartree-Fock contributions. Another convenient quantity for studying the pairing phases is the condensation energy, also called the correlation energy E_{corr} . This is defined as

$$E_{corr} = E_0 - E. \quad (5)$$

where E_0 is the energy of the ground state in the absence of a pairing condensate. The HFB ground state will maximize the correlation energy. By the Bloch-Messiah theorem [12, p. 611-612], the solution of the HFB equations could also be found by the BCS minimization with the variational wave function $|BCS\rangle = \prod_{\alpha} (u_{\alpha} + v_{\alpha} a_{\alpha}^{\dagger} a_{\bar{\alpha}}^{\dagger})|$, provided one knows the orbitals α and the pair correspondence $\alpha \rightleftharpoons \bar{\alpha}$. For ordinary spin-zero pairing in nuclei with even numbers of nucleons, we know that the pairs are the partner orbitals under the time-reversal operator. If the orbital basis does not have more than one orbital of given orbital angular momentum ℓ , the partners are related by the time-reversal operator, $|\bar{\alpha}\rangle = |\ell s j - j_z\rangle$ for $|\alpha\rangle = |\ell s j j_z\rangle$. Thus, for narrow energy-band windows

E_B and not too large nuclei, the BCS theory is adequate. This will provide one check on the more complicated HFB calculations.

For spin-triplet pairing in the presence of a spin-orbit field, the HFB treatment is unavoidable because the optimum orbital basis $|\alpha\rangle$ depends on the relative strengths of the pairing and spin-orbit fields. However, there is one case where the BCS treatment is valid. That is for a single j -shell and pairing in the $S_z = 0$ channel. In that case the pairing field demands that $j_z(\alpha) = -j_z(\bar{\alpha})$. This is uniquely satisfied by the same partnering as in the $S = 0$ pairing channel. We shall also use this case for testing the full HFB code.

Another important physical quantity is the quasiparticle energy E_q , defined as the eigenvalue of the HFB matrix equation, Eq. (6). It has the interpretation as the removal or addition energy for a particle in system with an even number of nucleons.

The $SU(4)$ limit

Before presenting calculations with physical values of the Hamiltonian parameters, we examine the theory in the limit of $SU(4)$ symmetry. The symmetry requires that the two pairing strengths be equal and that the potential be purely central. The HFB ground state of this Hamiltonian is highly degenerate, with many distinct ways to form the pairs. For example, one solution of the HFB equations is the state having both NN and PP pairing, with independent condensates for both. But we can equally well form a condensate pairing up-spin neutrons with up-spin protons and another condensate pairing the down-spin nucleons with each other. Both states have the same energy in the $SU(4)$ limit. This will be shown explicitly the example presented in Sect. IV. More generally, there is a continuous group of transformations that leaves the condensation energy invariant. The degeneracy of the HFB ground state can only be broken by treatments of the wave function beyond the HFB approximation, e.g. [23].

CALCULATIONAL DETAILS

We set up HFB equations in a basis of states $|i\rangle$ constructed from the eigenvectors of the central Hamiltonian $p^2/2m + V_{WS}F(r)$. We assume spherical symmetry and represent the orbital wave functions by their quantum numbers $i = (n, \ell, \ell_z, s_z)$ and radial wave functions $\phi_i(r)$ on a uniform radial mesh. The basis is truncated by keeping only states whose single-particle energies ε_ℓ (without spin-orbit) are within a range $E_B/2$ of the Fermi energy, $|\varepsilon_\ell - e_F| < E_B/2$. The spin-orbit interaction is treated by including its orbital interaction matrix elements in the HFB Hamiltonian.

To efficiently calculate the pairing field elements Δ_{ij} in the HFB matrix, we save and store the anomalous densities $\kappa_\alpha(r)$ on a radial grid. The densities ρ_{ij} and κ_{ij} are calculated in the orbital representation [12, p. 251, eq. (7.23)] from the selected columns of the transformation matrix that diagonalizes the HFB Hamiltonian. Under the assumption of spherical spatial symmetry, the HFB matrix is block-diagonal with respect to the orbital quantum number ℓ ; the different ℓ -blocks are calculated separately in our codes. If one restricts the anomalous density to channels having $S_z = 0$, the matrix can further be decomposed into blocks of fixed $|j_z| = |\ell_z + s_z|$. Further details are given in Appendix A.

RESULTS

An example: ^{48}Cr

Before applying the theory to very large nuclei, we investigated its performance in an experimentally well-studied region, namely the mass region corresponding to an open $f_{7/2}$ shell. The middle nucleus filling the $f_{7/2}$ shell is ^{48}Cr , with 4 neutrons and 4 protons outside the completely filled shells of $1s, 1p, 2s$, and $1d$ orbitals. To model this nucleus, we take the radius parameter $R = 4.62$ fm corresponding to the phenomenological The single-particle Hamiltonian gives a spectrum that corresponds very well with the shell assignments with the $f_{7/2}$ shell at the Fermi energy. The HFB equations are solved adjusting the chemical potential to get the correct particle number, $A = 48$. Some results for the HFB theory are presented in Table II, showing how the gaps and correlation energies depend on the Hamiltonian properties. We first demonstrate the degeneracy of HFB solutions when the Hamiltonian has $SU(4)$ symmetry in the spin and isospin degrees of freedom. The required Hamiltonian has spin-field set to zero and equal pairing strengths v_s and v_t . The calculated properties of the condensate are shown in the first four rows of Table II. One sees that the calculated quasiparticle energy is independent of the quantum numbers of the condensate and is the same for all orbitals. The correlation energy is also independent of the choice of condensate, demonstrating the degeneracy of the $SU(4)$ HFB ground state.

Going now to a more realistic Hamiltonian, rows 5 and 6 in the Table show the maximum effect of the spin-orbit field, taking only the $f_{7/2}$ shell for the single-particle space. Row 5 shows the results for an ordinary spin-singlet condensate, pairing neutrons with neutrons and protons with protons. The quasiparticle energy E_q is the same for all 8 orbitals in the shell. The value, $E_q \approx 1$ MeV, is in fact close to the average experimental odd-even mass difference. Row 7 shows the results for spin-triplet pairing. The $S = 1$ condensates define a direction in space and the gaps are no longer independent of the j_z

quantum number of the orbitals. These gaps are plotted as a function of j_z in Fig. 1. One sees that the gap approaches zero as j_z becomes small. This behavior would be called gapless superfluidity in a large system. The correlation energies of spin-singlet and spin-triplet pairing can be compared in the last column of the Table. One sees that it is smaller for spin-triplet than for spin-singlet. Thus, the ground state should exhibit ordinary pairing, as expected.

We next augment the single-particle space by adding the $f_{5/2}$ shell, including the physical spin-orbit splitting. The results for four choices of condensate are presented. First of all, one sees that the correlation energies are larger than in the pure $f_{7/2}$ Hamiltonian. They could not be smaller because the HFB theory is variational: enlarging the space can only lower the energy. The first two rows here show the results for spin-singlet pairing, differing on the isospin coupling. The energy are exactly the same due to the isospin invariance of the Hamiltonian. A similar degeneracy is found for the spin-triplet pairing; here the condensate energy does not depend on S_z . We shall exploit this invariance later by limiting our trial condensates to be either $(0, 1_0)$ or $(1_0, 0)$. Then j_z is conserved and the HFB matrix can be diagonalized in small blocks (See Appendix A). The final entry in the Table is for the Hamiltonian in the full fp -shell. This is in fact the truncation that result from the $E_B = 10$ MeV cutoff around the Fermi energy. We see that the correlation energies are larger, as expected. The spin-singlet pairing is still the stronger one, so the Hamiltonian with the E_B passes the test of agreeing with known phenomenology.

Systematics

In this section, we compare correlation energies for the triplet and singlet pairing channels as function of nuclear size. We showed in the previous section that the correlation energy does not depend on the z -components of the spin or isospin of the condensate, so we may limit our exploration of possible condensates to the $S_z = 0$ channels. As mentioned above, the HFB matrix reduces to blocks of fixed $|j_z|$ for these channels. We find the self-consistent solutions of the HFB equations iterating from a starting point in which there is a finite condensate in some channel.

For the range of nuclear sizes that we consider, the pairing gap is comparable to or smaller than the energy spacing of the shell orbitals. Under these conditions the strength of the pairing condensate will be quite sensitive to the Fermi level. Since we are interested here in nuclei that have well-formed pairing condensates, we shall only calculate systems where the chemical potential ($\lambda = -13$ MeV) coincides with the orbital energy of some j -shell. This gives about 50 cases for nuclei with radii in the

TABLE II: Pairing gaps and correlation energies for ^{48}Cr in the HFB theory. D is the dimension of the Δ or κ matrix; the dimension of the HFB matrix is twice that. The spin-singlet interaction strength is $v_s = 300$ MeV-fm³. The spin-triplet interaction strength is $v_t = 450$ MeV-fm³ except for the rows with the $SU(4)$ results; there $v_t = 300$ MeV-fm³. The condensates are labeled by the spin-isospin quantum numbers, dropping the z -quantum number when $S = 0$ or $T = 0$. The column marked E_q gives the value or the range of values of the quasiparticle energy of orbitals at the Fermi energy. The correlation energy E_{corr} in the last column is defined in eq. (5).

Space	D	condensate (S_{S_z}, T_{T_z})	E_q (MeV)	E_{corr} (MeV)
f -shell $SU(4)$	28	$(0, 1_1), (0, 1_{-1})$	1.80	10.27
		$(0, 1_0)$	1.80	10.27
		$(1_1, 0), (1_{-1}, 0)$	1.80	10.27
		$(1_0, 0)$	1.80	10.27
$f_{7/2}$	16	$(0, 1_1), (0, 1_{-1})$	1.03	4.11
		$(0, 1_0)$	1.03	4.11
		$(1_0, 0)$	0.12-0.87	2.01
$f_{7/2}, f_{5/2}$	28	$(0, 1_1), (0, 1_{-1})$	1.16	4.64
		$(0, 1_0)$	1.16	4.64
		$(1_1, 0), (1_{-1}, 0)$	0.20-1.34	2.98
		$(1_0, 0)$	0.20-1.34	2.98
full fp	28 + 12	$(0, 1_1), (0, 1_{-1})$	1.23	4.92
		$(0, 1_0)$	1.23	4.92
		$(1_1, 0), (1_{-1}, 0)$	0.26-1.58	3.45
		$(1_0, 0)$	0.26-1.58	3.45

range of 4.0-12.0 fm. These correspond to mass numbers in the range $A = 25 - 1000$. A table of the results for the two correlation energies and their ratio is given in Appendix B. For the lighter nuclei, correlation energies are of the order of several MeV, except for several nuclei with $j = 1/2$ shells at the Fermi level, for which the spin-singlet correlation energy can be less than 1 MeV. In the heavy nuclei, the correlation energy can be several tens of MeV.

Fig. 2 shows a plot of the ratio of spin-triplet to spin-singlet correlation energies as a function of the mass A . The results show that there is a trend to favor spin-triplet pairing for large nuclei, as was argued in the Introduction. However, the ratio is by no means monotonic as a function of R . Spin-singlet is favored for $R < 6.5$ fm and spin-triplet for $R > 9$ fm, but nuclei in between could have either ground state. The lightest nuclei predicted to have spin-triplet condensates are indicated by their mass and element designation. They are ^{30}P , ^{76}Sr , and ^{136}Er . The two lighter ones are in the physical region, and the spectroscopic properties of one of them, ^{30}P , are well-known. The calculated correlation energy for this nucleus is 1.4 MeV, which is not large enough to be considered a strong condensate. Nevertheless, the observed

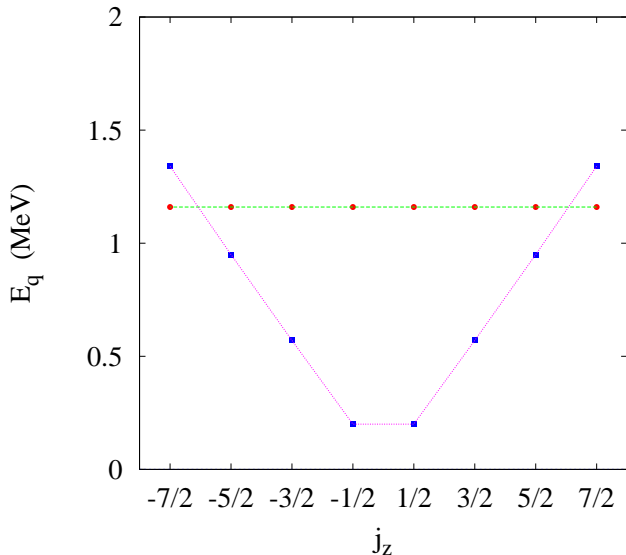


FIG. 1: Quasiparticle energies in ^{48}Cr for the f -shell space. Red circles: spin-singlet; blue squares: spin-triplet with condensate in the $S_z = 0$ channel. Lines are drawn to guide the eye.

ground state spin and parity ($J^\pi = 1^+$) agrees with the quantum numbers of the spin-triplet condensate. The middle nucleus, ^{76}Sr has a somewhat smaller condensation energy, $E_{cor} \approx 1$ MeV, so any effects of the pairing would be quite weaker. The nuclei in this mass region are accessible with current-generation accelerators and their experimental spectroscopic properties are under active study. The third nucleus, ^{136}Er , just beyond the physical region, is the smallest nucleus having both strong pairing ($E_c \sim 13$ MeV) and a spin-triplet condensate. There are two nearly degenerate shells at the Fermi energy, the $2s_{1/2}$ and $1d_{3/2}$ shells. They both have radial nodes and weak spin-orbit splitting from their j -shell partners.

A table of the correlation energies is given in Appendix B. The table also shows the angular momentum quantum numbers at the Fermi energy for each case calculated.

CONCLUSION

This study offers a resolution of the conundrum, why is it that ordinary nuclei only exhibit spin-singlet pairing when nuclear matter calculations find that spin-triplet pairing is stronger? The answer, that ordinary nuclei are too small to be out of the influence of the surface spin-orbit field, is seen by calculating the pairing energies over a large range of sizes. For our Hamiltonian, the spin-triplet pairing dominates for all calculated nuclei whose radii are larger than ~ 9 fm, and for a number of lighter nuclei having low- l shells at the Fermi energy. The candidate for the smallest nuclei with a well-developed condensate, $A \sim 130 - 140$, is tantalizingly close to region of

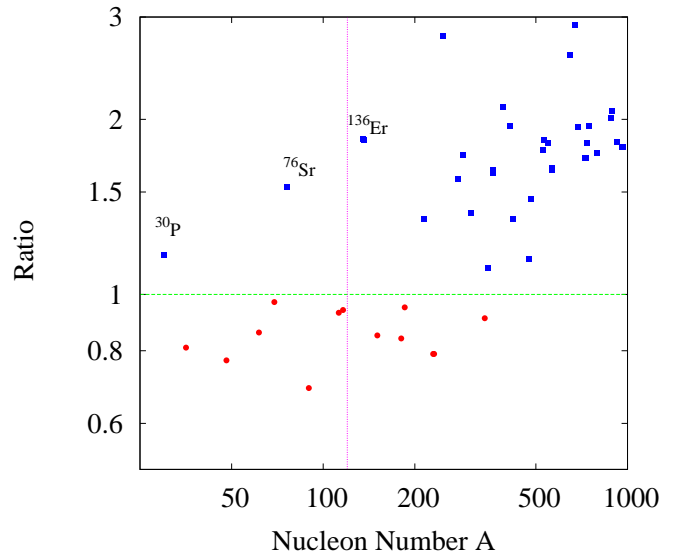


FIG. 2: Ratio of spin-triplet to spin-singlet correlation energies as a function of mass number A . Nuclei with spin-singlet and spin-triplet condensates are shown as red circles and blue squares, respectively. The vertical line at $A \approx 120$ shows the dividing line between nuclei that are bound (left) and nuclei that unstable with respect to proton emission, according to the mass table of ref. [13].

physical nuclei defined by the single-nucleon driplines.

However, due to the simplifications made to the Hamiltonian and to other uncertainties we cannot be quantitative about the transition point. In particular, important physics may be lost in ignoring the momentum- and density-dependence of the pairing interaction. In the theory of nuclear matter the spin-singlet pairing derived from Brueckner theory is very weak at nuclear matter density [14, See Fig. 8][15]; see also the contradicting claim in ref. [16]. The pair gap becomes larger at subnuclear densities, suggesting that surface effects are crucial for that channel. In many studies of nuclear structure, the authors assume that there is some surface enhancement of the pairing, see e.g. [17, 18, 19]. Beyond the effects that are treated in the Brueckner theory, there is likely to be a significant induced interaction associated with collective surface vibrations [20]. If we included either mechanisms enhancing the surface region, the pairing energy would decrease as the nucleus becomes larger. This of course could effect the crossover from singlet to triplet condensates. Also one needs to take into account renormalization effects associated with the truncation of the orbital space. One finds that the renormalized interaction is actually suppressed in the surface region [21]. Clearly, there is much left to do to improve the interaction.

It would also be interesting to explore the effects of nuclear deformation. Breaking the spherical symmetry would effectively reduce the single-particle level density

at mid-shell filling, weakening the pairing condensates. How this affects the competition between the two kinds of pairing is not known.

There are a number of other questions that could be addressed within the context of the simplified Hamiltonian that we have employed. Can two kinds of condensates coexist in the same system? At first sight this seems unlikely because the bulk pair correlation length is large compare to the sizes of the nuclei we consider. However, it has been claimed that the Cooper pairs have a small size in the nuclear surface[22]. This might allow the existence of a mixed phase with a strong spin-triplet condensate in the interior and a spin-singlet condensate on the surface. Another interesting question is the fragility of spin-triplet pairing is when there is a neutron excess. For our midmass triplet-pairing candidate nucleus, $N = Z \sim 65$, the condensate seems quite robust with a calculated correlation energy 6 MeV larger than the singlet energy. It might be that the system could support a few excess neutrons and still preserve the triplet condensate.

We have not addressed the question of how the triplet pairing condensate could be observed, beyond noting that the character of the condensate controls quantum numbers of the ground state in an odd-odd system. In fact several $J = 1, T = 0$ ground states are sprinkled among the 12 odd-odd $N = Z$ nuclei known experimentally. The β -decay spectrum may also be affected by the pairing[23]. Finally, two-particle transfer reactions would be affected by the coherence of the pairing fields.

The authors thank M. Horoi for supplying us with the GX1A interaction. We also thank A. Bulgac, T. Duguet, B. Spivak and S. Baroni for discussions, and J. Vinson for help in an early stage of this work. This work was supported by DOE Grant DE-FG02-00ER41132.

Appendix A

The Hartree-Fock-Bogoliubov equations have the general structure

$$\begin{bmatrix} H_{sp} - \lambda \mathbf{1} & \Delta \\ -\Delta^* & -H_{sp} + \lambda \mathbf{1} \end{bmatrix} \begin{pmatrix} u_\alpha \\ v_\alpha \end{pmatrix} = E_\alpha \begin{pmatrix} u_\alpha \\ v_\alpha \end{pmatrix}. \quad (6)$$

Here H_{sp} and Δ are matrices in some basis of orbital wave functions and u_α, v_α are column vectors. The ordinary and anomalous density matrix elements are given by

$$\rho_{ij} = \sum_\alpha v_{\alpha,i}^* v_{\alpha,j} \quad (7)$$

$$\kappa_{ij} = \sum_\alpha u_{\alpha,i}^* v_{\alpha,j}$$

where the sums are restricted to eigenvectors satisfying $E_\alpha > 0$. We construct the HFB matrix assuming that

the nucleus is spherical with spherically symmetric fields except for the spin variables, using as a basis of the orbital wave functions the eigenfunctions of the central potential which may be labeled by the quantum numbers $(n, \ell, \ell_z, s_z, t_z)$.

To efficiently calculate the pairing field elements Δ_{ij} in the HFB matrix, we save and store the anomalous densities $\kappa_\alpha(r)$ on a radial grid. The densities are defined

$$\kappa_\alpha(r) = \frac{1}{4\pi} \sum_{i>j} \phi_i(r) \phi_j(r) \langle \alpha | ij \rangle \kappa_{ij} \quad (8)$$

where

$$\langle ij | \alpha \rangle = \sqrt{2} ((1/2 s_{zi} 1/2 s_{zj} | S_\alpha S_{z\alpha}) \times \quad (9)$$

$$(1/2 t_z(i) 1/2 t_z(j) | T(\alpha) T_z(\alpha)) (-)^{\ell_i - \ell_{zi}} \delta_{\ell_i, \ell_j} \delta_{\ell_{zi}, \ell_{zj}}.$$

and the radial wave functions ϕ_i are normalized as $\int_0^\infty r^2 dr |\phi_i(r)|^2 = 1$. The elements of the HFB Δ matrix are calculated as

$$\Delta_{ij} = \sum_\alpha \langle ij | \alpha \rangle v_\alpha \int_0^\infty r^2 dr \phi_i(r) \phi_j(r) \kappa_\alpha(r). \quad (10)$$

where v_α is the strength of the contact interaction defined in eq. (3).

Due to the symmetry, the condensation energies can be calculated under the further assumption that the total azimuthal angular momentum $|j_z| = |\ell_z + s_z|$ is conserved. The HFB matrix then decomposes into 2×2 or 4×4 dimensional blocks with respect to spin and orbital angular momentum s_z and $\ell - z$. A typical subblock for a fixed isospin of the pairing field has the form

$$\begin{bmatrix} \mathbf{h}_{\ell, j_z} - \lambda \mathbf{1} & 0 & 0 & \Delta_\ell \\ 0 & \mathbf{h}_{\ell, -j_z} - \lambda \mathbf{1} & -\Delta_\ell & 0 \\ 0 & -\Delta_\ell & -\mathbf{h}_{\ell, j_z} + \lambda \mathbf{1} & 0 \\ \Delta_\ell & 0 & 0 & -\mathbf{h}_{\ell, -j_z} + \lambda \mathbf{1} \end{bmatrix} \quad (11)$$

Assuming that there is only one radial state in the E_B window, the \mathbf{h} and Δ matrices have dimension 1 or 2 depending on whether $|j_z| = \ell + 1/2$ or not. In the latter case, the \mathbf{h}_{ℓ, j_z} matrix is given by

$$\mathbf{h}_{\ell, j_z} = \begin{bmatrix} \varepsilon_\ell + (j_z - 1/2)w_\ell/2 & \sqrt{(\ell + 1/2)^2 - j_z^2}w_\ell/2 \\ \sqrt{(\ell + 1/2)^2 - j_z^2}w_\ell/2 & \varepsilon_\ell - (j_z + 1/2)w_\ell/2 \end{bmatrix} \quad (12)$$

where ε_ℓ is the orbital energy calculated without the spin-orbit field and w_ℓ is the radial matrix element of the spin-orbit field. The matrix Δ_ℓ is given by

$$\Delta_\ell = \begin{bmatrix} 0 & d_\ell \\ \pm d_\ell & 0 \end{bmatrix}. \quad (13)$$

Here the upper and lower signs apply to the $(ST) = (01)$ and (10) channels, respectively. The pairing field d_ℓ is identical to Δ_{ij} in eq. (10) with eg. $|i\rangle = |n\ell\ell_z s_z t_z\rangle$ and

$|j\rangle = |n\ell - \ell_z - s_z - t_z\rangle$. Note that d_ℓ is the same for all the HFB subblocks of given ℓ . The 2×2 HBF matrix in the $|j_z| = \ell + 1/2$ case can be obtained by eliminating the orbitals with unphysical m values from the basis.

To solve the HFB equations, we start with a trial field for the anomalous density $\kappa_\alpha(r)$, typically a constant value independent of r in some channel α and zero in the other channels. The solution of the HFB equation with the trial field is used to calculate a new field, and the process is iterated to convergence.

A computer code to solve the HFB equations based on these formulas is available by E-mail from the authors, bertsch@u.washington.edu.

Appendix B

Columns in the table refer to:

R , the radius parameter of the Woods-Saxon potential eq. (2)

A , the nuclear mass number

$E_c(s)$, the spin-singlet condensation energy in MeV

$E_c(t)$, the spin-triplet condensation energy

$R_{ts} = E_c(t)/E_c(s)$, their ratio

ℓ, j , orbital and total angular momentum of the single-particle orbital at the Fermi energy.

R	A	Ec(s)	Ec(t)	R-ts	l	j
4.14	29.9	1.3	1.5	1.17	0	1/2
4.28	35.4	2.4	2.0	0.81	2	3/2
4.77	48.1	4.8	3.7	0.77	3	7/2
5.20	61.5	2.8	2.4	0.86	1	3/2
5.30	69.1	4.4	4.3	0.97	3	5/2
5.40	76.2	0.9	1.3	1.53	1	1/2
5.70	89.7	5.1	3.5	0.69	4	9/2
6.24	112.5	5.9	5.5	0.93	2	5/2
6.27	116.2	6.6	6.2	0.94	4	7/2
6.50	135.1	7.0	12.9	1.85	0	1/2
6.51	135.7	7.0	12.9	1.84	2	3/2
6.62	150.6	6.5	5.6	0.85	5	11/2
7.21	180.5	6.6	5.6	0.84	5	9/2
7.24	185.3	5.8	5.6	0.95	3	7/2
7.51	214.8	13.5	18.3	1.35	6	13/2
7.57	229.8	7.4	5.8	0.79	3	5/2
7.58	231.5	7.3	5.8	0.79	1	3/2
7.72	247.3	0.8	2.3	2.78	1	1/2
8.13	276.8	9.5	15.0	1.58	6	11/2
8.23	287.0	9.8	17.1	1.74	4	9/2
8.39	305.1	11.8	16.3	1.38	7	15/2
8.60	339.5	3.9	3.6	0.91	4	7/2
8.64	346.6	3.3	3.6	1.11	2	5/2
8.84	360.9	1.9	3.1	1.62	2	3/2
8.85	361.5	1.8	3.0	1.64	0	1/2
9.03	390.8	12.3	25.7	2.10	7	13/2
9.19	410.7	15.7	30.5	1.95	5	11/2
9.26	420.9	14.0	18.8	1.35	8	17/2

9.60	474.1	4.2	4.9	1.15	5	9/2
9.68	481.9	3.7	5.4	1.46	3	7/2
9.92	528.0	17.9	31.6	1.77	8	15/2
9.95	532.8	16.7	30.7	1.84	1	3/2
10.05	549.8	19.7	35.8	1.82	1	1/2
10.13	562.8	23.2	38.0	1.64	9	19/2
10.14	564.5	22.9	37.8	1.65	6	13/2
10.57	647.2	7.2	18.5	2.58	6	11/2
10.69	669.4	11.4	33.1	2.91	4	9/2
10.79	688.8	16.5	32.1	1.94	9	17/2
10.97	726.2	27.5	47.3	1.72	4	7/2
10.98	728.2	27.5	47.2	1.72	10	21/2
10.99	730.3	27.3	47.0	1.72	4	7/2
11.03	738.6	24.8	45.1	1.82	2	5/2
11.07	747.1	21.1	41.1	1.95	7	15/2
11.18	791.4	10.2	18.0	1.75	2	3/2
11.53	854.6	10.8	36.9	3.41	7	13/2
11.66	882.0	22.6	45.3	2.01	10	19/2
11.69	888.4	21.8	45.0	2.07	5	11/2
11.83	920.2	19.1	34.9	1.83	11	23/2
11.99	960.7	18.3	32.7	1.79	8	17/2
12.00	963.2	18.2	32.6	1.79	5	9/2

-
- [1] A.O. Macchiavelli, et al., Phys. Rev. C **61** 041303R (2000).
 - [2] A.O. Macchiavelli, et al., Phys. Lett. B **480** 1 (2000).
 - [3] A. Poves and G. Martinez-Pinedo, Phys. Lett. B **430** 203 (1998).
 - [4] G.F. Bertsch and S. Baroni, arXiv:0904.2017.
 - [5] G.F. Bertsch, A.O. Macchiavelli, and A. Schwenk, unpublished; see also S. Baroni, A.O. Macchiavelli, and A. Schwenk, arXiv:0912.0697.
 - [6] This may be contrasted with the situation in condensed matter physics: the electronic spin-orbit field does not affect the condensation energy. See e.g. A. Fetter and P. Hohenberg, in "Superconductivity", ed. R.D. Parks, (Marcel Dekker, 1969), vol. II, p. 882.) The difference is that the nuclear spin-orbit field affects the density of states at the Fermi level, but the electronic spin-orbit is too weak to do so in metals.
 - [7] A. Bohr and B. Mottelson, "Nuclear Structure," (Benjamin, 1969), Volume I.
 - [8] In particular, the nucleon-nucleon tensor interaction contributes to the splittings of spin-orbit partners, but with a different radial dependence than that arising from the nucleon-nucleon spin-orbit interaction. See B. A. Brown, T. Duguet, T. Otsuka, D. Abe, T. Suzuki, Phys. Rev. C **74** 061303 (2006).
 - [9] Y. Uozumi, et al. Phys. Rev. C **50** 263 (1994).
 - [10] B.A. Brown and W.A. Richter, Phys. Rev. C **74** 034315 (2006).
 - [11] M. Honma, T. Otsuka, B.A. Brown, and T. Mizusaki, Eur. Phys. J. A **25** Suppl. 1,499 (2005); Phys. Rev. C **69** 034335 (2004).
 - [12] P. Ring and P. Schuck, "The nuclear many-body problem", (Springer, 1980).

- [13] P. Moller, et al., At. Data Nucl. Data Tables **9** 185 (1995).
- [14] M. Baldo, et al., Nucl. Phys. **A515** 409 (1990).
- [15] E. Garrido, et al., Phys. Rev. C **63** 037304 (2001).
- [16] O. Elgaroy, L. Engvik, M. Hjorth-Jensen, and E. Osnes, Phys. Rev. Lett. **77** 1428 (1996); Phys. Rev. C **57** R1069 (1998).
- [17] J. Terasaki, et al., Nucl. Phys. **A593** 1, (1995).
- [18] J. Dobaczewski, W. Nazarewicz, and P.-G. Reinhard, Nucl. Phys. **A693** 361 (2001).
- [19] N. Sandulescu, P. Schuck, and X. Vinãs, Phys. Rev. C **71** 054303 (2005).
- [20] A. Pastore, et al., Phys. Rev. C **78** 024315 (2008).
- [21] Y. Yu and A. Bulgac, Phys. Rev. Lett. **90** 222501 (2003).
- [22] N. Pillet, N. Sandulescu, and P. Schuck, Phys. Rev. C **76** 024310 (2007).
- [23] J. Engel, S. Pittel, M. Stoitsov, P. Vogel, and J. Dukelsky, Phys. Rev. C **55** 1781 (1995).